ICARUS **135,** 451–457 (1998)
ARTICLE NO. IS985991

Photometric Properties of Asteroid 4179 Toutatis from Lightcurves and a Radar-Derived Physical Model

R. Scott Hudson

School of Electrical Engineering and Computer Science, Washington State University, Pullman, Washington 99164-2752
E-mail: hudson@eecs.wsu.edu

and

Steven J. Ostro

Jet Propulsion Laboratory, California Institute of Technology, Pasadena, California 91109-8099

Received December 15, 1997; revised June 1, 1998

Optical lightcurves reported by J. R. Spencer *et al.* (1995, *Icarus* 117, 71–89) and a radar-derived shape and spin-state model (R. S. Hudson and S. J. Ostro, 1995, *Science* 270, 84–86) are used to estimate the Hapke parameters of the Earth-crossing Asteroid 4179 Toutatis. We find a particle single-scattering albedo $w = 0.261 \pm 0.019$, opposition surge width $h = 0.036 \pm 0.023$ and amplitude $B_0 = 1.20 \pm 0.32$, particle phase function asymmetry factor $g = -0.29 \pm 0.06$, and macroscopic roughness parameter $\bar{\theta} = 32 \pm 8°$. The synthetic lightcurves generated with this model provide a good fit (rms residual = 0.12 mag) to the optical data which span phase angles from 0.2° to 121.4°. The addition of optical data in the modeling process results in a slight refinement of the radar-derived estimate of the parameters that describe Toutatis's non-principal-axis spin state. Analysis of the opposition surge width in light of recent radar results supports the hypothesis that a significant fraction of Toutatis's surface is covered by a fine particulate regolith.

Key Words: **asteroids; photometry; radar; surfaces.**

INTRODUCTION

An asteroid's optical lightcurve carries substantial information about the physical properties of the object. However, since a lightcurve depends on the asteroid's shape, spin-state, and photometric properties in complex way, it is generally not possible to separate these effects in a detailed manner without additional information. The most difficult property to constrain using lightcurves is probably shape, so significant leverage for lightcurve interpretation can be gained if an independently derived shape model is available.

In the case of the mainbelt asteroids Gaspra and Ida, Galileo optical images have been used to produce shape models (Thomas *et al.* 1994, 1996a) that in turn have been used to interpret groundbased lightcurves (Simonelli *et al.* 1995, 1996) and the spatially resolved spacecraft images (Helfenstein *et al.* 1994, 1996). In both cases global-average values of five Hapke photometric model parameters were estimated. Lightcurve fits were accurate to about 0.05 mag over phase angles of 0.6°–24.9° for Gaspra and 1.4°–15.6° for Ida. No evidence of large variations in photometric properties across the surfaces was found.

Currently radar is the only source of spatially resolved images of Earth-crossing asteroids (ECAs). Because radar wavelengths are some five orders of magnitude larger than optical wavelengths, the images do not themselves carry information about the optical photometric properties of a body's surface although they do carry information about its radar scattering properties. Therefore, even with the availability of high resolution radar images, groundbased lightcurves are our only source of information about the optical photometric properties of ECAs.

The ability to produce shape models from radar images has been demonstrated in the case of the ECAs Castalia (Hudson and Ostro 1994) and Toutatis (Hudson and Ostro 1995). In Castalia's case the synthesis of radar and optical data into a unified physical model has been demonstrated (Hudson *et al.* 1997). In this paper we extend this type of analysis to the S-class (Howell *et al.* 1994) ECA Toutatis.

Toutatis is an interesting object on several accounts. With a maximum dimension of 4.6 km it is one of the largest ECAs, and it is to date the only asteroid unmistakably identified as being in a non-principal-axis spin state (Hudson and Ostro 1995). The 0.46° inclination of Toutatis's extremely chaotic orbit is the smallest of any known ECA, and its 1:4 resonance with the Earth results in close approaches every four years (Whipple and Shelus 1993, Yeomans and Chodas 1994).

0019-1035/98 $25.00

Because of the detailed nature of the Toutatis shape model and the extensive nature of the Toutatis lightcurves, the procedure described below also serves as a test case for how well Hapke parameters can be determined from groundbased observations.

PHYSICAL MODEL AND DATA SETS

During 1992 and 1993 Toutatis was the subject of an extensive campaign of optical (Spencer *et al.* 1995) and radar (Ostro *et al.* 1995) observations. The optical data spanned solar phases between 0.2° and 121.4°, providing the most extensive phase coverage obtained for any asteroid to date. Here we make use of the published V magnitude values ($H(\alpha)$) of Spencer *et al.*. Strong minima occurred approximately every 7.3 days, but the lightcurve was not well fit by a single rotation period. Spencer *et al.* concluded that the object has a complex rotation state.

Over 19 consecutive days during December 1992, Ostro *et al.* imaged Toutatis with the Goldstone and Arecibo radar systems. The resulting images constitute the finest resolution and highest SNR asteroid radar data set obtained to date. Using these radar images, Hudson and Ostro (1995) reconstructed Toutatis's shape and spin state. Their model revealed a very irregular, elongated object of effective diameter 2.45 km in a non-principal-axis spin state characterized by periods of 5.41 and 7.35 days.

METHOD AND RESULTS

We applied a Hapke photometric model with a one-parameter Henyey–Greenstein phase function (Hapke 1981, 1984, 1986; Hapke 1993; see Eqs. (12.55) and (6.7) therein) to the radar-derived Toutatis shape and spin-state model. Starting with the radar-derived spin state and "average S-type asteroid" Hapke parameters (Helfenstein *et al.* 1996), a χ^2 minimization as described by Hudson *et al.* (1997) produced estimates of the five Hapke parameters and eight spin-state parameters. Because the time base of the optical observations is much greater than that of the radar observations (Fig. 1) we might expect that the optical data could provide some refinement to the spin state. Three of the spin-state parameters are Euler angles (Landau and Lifshitz 1976) (ϕ_0, θ_0, ψ_0) that orient the asteroid with respect to ecliptic coordinates at time t_0. The first two orient the object's long axis and the third describes the asteroid's orientation about that axis. Three other parameters (ω_{0s}, ω_{0i}, ω_{0l}) are the projections of the spin vector along the three principal axes (short, intermediate, long, respectively) at t_0 and two parameters describe the ratios of the moments of inertia. (The absolute value of the moments would require knowledge of the asteroid's mass.)

The resulting spin state parameters are shown in Table I. A formal covariance calculation yielded uncertainty estimates similar to those resulting from the radar data, so we retain the uncertainties quoted by Hudson and Ostro (1995). The changes in the spin-state parameters due to folding in lightcurves are less than the parameter uncertainties except in the case of ψ_0. This angle specifies the initial orientation of the asteroid about its long axis, and its estimate is correlated with the initial values of the two compo-

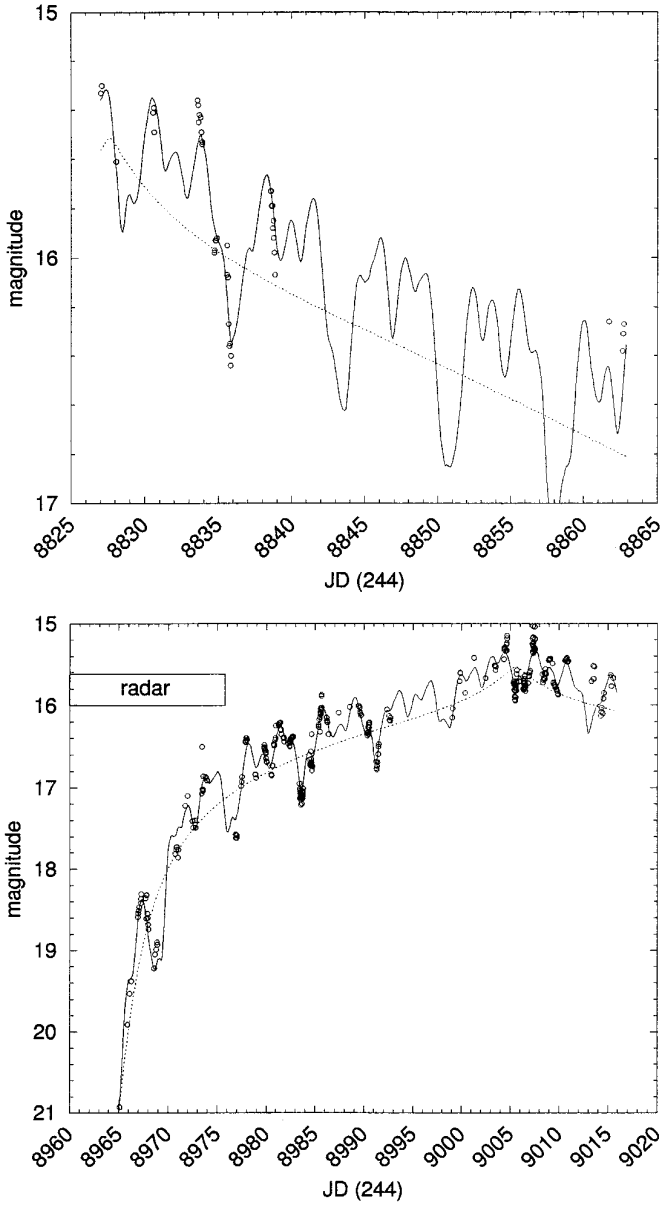

FIG. 1. Toutatis lightcurve fits (top, Jul./Aug. 1992; bottom, Dec. 1992/Jan. 1993). The circles are observed $H(\alpha)$ data from Spencer *et al.* (1995), the solid line is the synthetic lightcurve of the Toutatis model, and the dotted line is the lightcurve of a 2.45-km-diameter sphere with the same Hapke parameters. The bar labeled "radar" indicates the duration of radar observations. Note that the plots have different scales. The rms error is 0.12 mag.

TABLE I
Toutatis Spin State, 11 Dec. 1992, 9:21 UTC

	ϕ_0	θ_0	ψ_0	ω_{0s}	ω_{0i}	ω_{0l}	I_s/I_l	I_i/I_l
Radar	−103°	94°	−136°	20°/day	32°/day	98°/day	3.19	3.01
Radar + optical	−103°	91°	−129°	21°/day	31°/day	98°/day	3.22	3.02
Uncertainty	±3°	±3°	±3°	±1°/day	±1°/day	±1°/day	±0.1	±0.1

nents of the spin vector that are orthogonal to the long axis. These sorts of interactions between three parameters are not accounted for when using the covariance matrix to calculate uncertainties (which considers only pair-wise correlations).

Figure 1 shows the lightcurve fits. The top and bottom data are separated by approximately 100 days. The dotted curves show the brightness of a 2.45-km-diameter sphere with the same Hapke parameters illustrating the contribution of phase effects separate from shape and spin state. Both sets pass through nearly 0° phase as marked by the opposition spike in the dotted curves. The July/August data extend from 0.5° to 34.0° of phase, while the December/January data extend from 0.2° to 121.4°. The rms error of the fit is 0.12 mag.

The estimated Hapke parameters are listed in Table II together with parameters of other asteroids and Phobos and Deimos for comparison. A primary rationale behind estimating photometric parameters is to enable physical inferences to be made about the composition and structure of a body's surface and to provide a quantitative basis for comparing the surfaces of different objects. Several authors have pointed out that reliable determination of photometric parameters from disk-integrated data requires observations over a wide range of solar phases, e.g., from <2° to >90° (Veverka 1977, Helfenstein 1988, Bowell *et al.* 1989).

Thus comparative work among asteroids can be problematic because of varying degrees of uniqueness and indeterminacy for the different targets, for which Hapke parameters have been derived from different combinations of spatially resolved and disk-integrated data that provide different degrees of phase-angle coverage. Therefore we paid considerable attention to the question of how well the individual parameters could be constrained. The spin state parameters were frozen at the best-fit solution and one-by-one the Hapke parameters were forced to step through given values, while the other four were allowed to vary. In this manner the full nature of inter-parameter

TABLE II
Hapke Parameters of Selected Small Bodies

Object	Data	Phases	Particle albedo, w	Opposition surge		Asymmetry parameter g	Macroscopic roughness $\bar{\theta}$
				Width, h	Amplitude, B_0		
Toutatis	EB	0°–121°	0.261 ± 0.019	0.036 ± 0.023	1.20 ± 0.32	−0.29 ± 0.06	32° ± 8°
Ida[a]	EB	1°–21°	$0.218^{+0.024}_{-0.005}$	0.020 ± 0.005	1.53 ± 0.10	−0.33 ± 0.01	18° ± 2°
	GL	20°–110°					
Dactyl[a]	GL	20°–26°	$0.211^{+0.028}_{-0.010}$	[0.020]	[1.53]	−0.33 ± 0.03	23° ± 5°
Gaspra[a]	EB	2°–25°	0.360 ± 0.07	0.060 ± 0.01	1.63 ± 0.07	−0.18 ± 0.04	29° ± 2°
	GL	33°–51°					
Ave S-ast.[a]	EB	<30°	0.23	0.02	1.32	−0.35	[20°]
Castalia-N[b]	EB	58°–90°	0.384 ± 0.07	—	—	−0.11 ± 0.09	46° ± 10°
Castalia-S[b]	EB	58°–90°	0.239 ± 0.07	—	—	−0.30 ± 0.09	25° ± 10°
Apollo[c]	EB	0°–89°	0.318 ± 0.004	0.034 ± 0.007	0.90 ± 0.02	−0.32 ± 0.01	15° ± 1°
Phobos[d]	VK	1°–123°	0.070 ± 0.020	0.055 ± 0.025	4.0^{+6}_{-1}	−0.08[f]	22° ± 2°
Deimos[e]	VK	1°–81°	$0.079^{+0.008}_{-0.006}$	$0.068^{+0.082}_{-0.037}$	$1.65^{+0.90}_{-0.61}$	−0.29 ± 0.03	16° ± 5°

Note. EB, Earth-based (V filter); GL, Galileo (GRN filter); VK, Viking (clear filter).
[a] Hefenstein *et al.* 1996.
[b] Hudson *et al.* 1997.
[c] Hefenstein and Veverka 1989.
[d] Simonelli *et al.* 1998.
[e] Thomas *et al.* 1996.
[f] Effective value for two-term Henyey–Greenstein phase function.

correlations of arbitrary order could be examined. The Toutatis parameter uncertainties we derived in this manner are shown in Table II.

Our estimates of Toutatis's Hapke parameters fall between that of the S-class Asteroid Gaspra and that of S-class Asteroid Ida except that B_0 (the amplitude of the opposition effect) is smaller and $\overline{\theta}$ (the macroscopic roughness) is somewhat larger for Toutatis, although the differences are within the uncertainties. (Note: JPL's Solar System Visualization group has an MPEG animation of Toutatis rotating as its lightcurve develops; see http://www-ssv.jpl.nasa.gov/SSV/ast_clips.html. Other renderings are available at http://www.eecs.wsu.edu/~hudson/asteroids.html.)

DISCUSSION

Lightcurve Residuals

The Toutatis rms error of 0.12 mag is considerably more than the ~0.05-mag rms error that characterizes lightcurve fits obtained with Galileo-based models of Gaspra and Ida (Simonelli *et al.* 1995, 1996). What does this mean?

For a principal-axis rotator in the main belt, brightness variations are essentially periodic. This results in a considerable amount of redundancy during, say, a given apparition, so a few individual periods can well represent an entire data set. Consequently it was reasonable for Simonelli *et al.* to limit their Ida lightcurve analysis to four selected lightcurves representing "high-quality observations having low internal scatter," and in the case of Gaspra to have "analyzed only a carefully selected subset of the available data."

For Toutatis, a non-principal-axis (hence nonperiodic) rotator exhibiting a rapidly varying phase angle, such redundancy does not occur. Consequently, one cannot select segments of the data set without the real possibility of throwing away unique information. Therefore, in the current analysis we chose to use all the published observations (371 data), representing 45 observers and 26 observatories, without any preselection process. The large number of observatories involved increases the possibility that systematic errors might be a problem in fitting all the data with a single physical model. For example, in their description of Gaspra photometry, Wisniewski *et al.* (1993) noted that "There seem to be significant inconsistencies between data from different observatories." Such inconsistencies will probably not be represented in the stated uncertainties. In light of this, we chose to weight all data equally in the fit regardless of their stated uncertainties.

As an illustration of the kind of individual residuals that contribute to the 0.12-mag rms error, Fig. 2 shows expanded views of the fit over about 13 days from JD 2449003 until the end of observations. Two kinds of residuals are apparent.

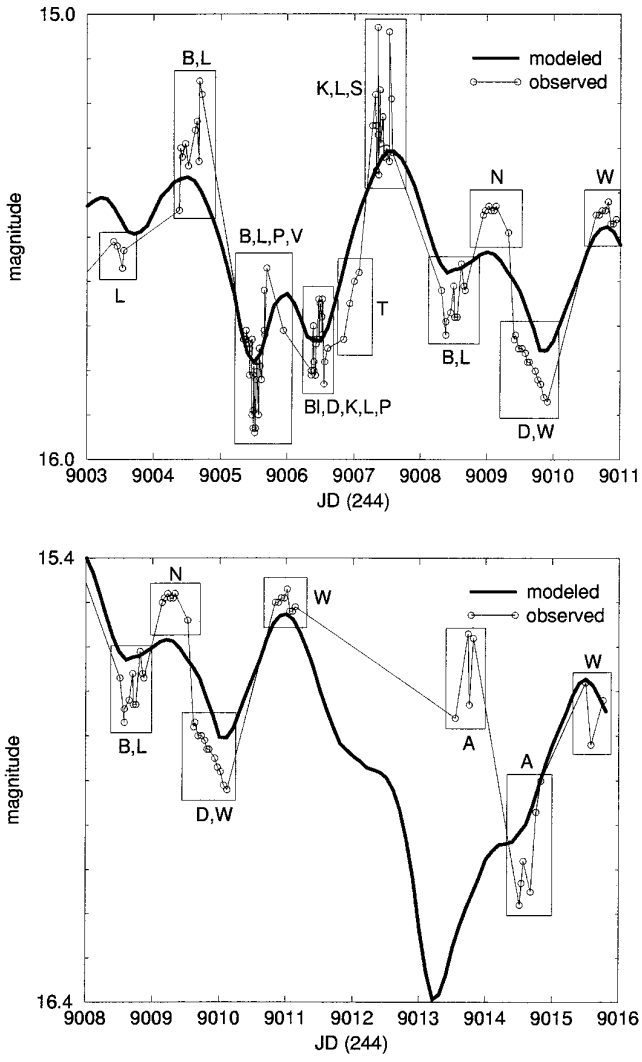

FIG. 2. Detail of Toutatis lightcurve fits over approximately last 13 days of observations. Data are grouped by boxes and labeled according to observers listed in Table III of Spencer *et al.* (1995).

One type is represented by blocks "B,L,P,V" and "K,L,S." These display rapid variations that are generally much larger than the stated uncertainties (Spencer *et al.* 1995, Table III). The time scale of these variations is so short that it does not seem possible to understand them in terms of shape and/or spin state errors or in terms of the Hapke photometric model. Most likely these residuals are overwhelmingly dominated by errors in the data.

The other type of residual is represented by blocks "T", "N", and "D,W" in which the observed data generally have the same shape as the modeled data but are offset in magnitude. In this case it would seem more reasonable that the residuals could point to errors in the spin state, shape model, or photometric model. Given that the spin state was free to change during these fits, no statistically

significant errors should result from differences between the modeled and true spin states. So the most likely sources of modeling error are shape and photometric function.

Three considerations argue against an explanation of these residuals in terms of shape errors. First, the lightcurve is only slightly sensitive to shape changes that are large enough to visibly degrade the shape model's fit to radar images. We verified this by examining radar and optical fits with a perturbed shape model. Second, one might expect that errors in the shape model would lead to the observed and modeled lightcurves having different shapes themselves. However, in fact, in these "offset" residuals the observed and modeled lightcurves generally agree in shape over, for example, a single day but display varying offsets between different days and/or between different observers. Third, the current shape model was able to fit new (1996) Goldstone radar images (Ostro *et al.* 1998).

We tested the possibility that these residuals might be the result of "overextending" the Hapke model by using a single set of parameters over ~120° of solar phase. (For example, Simonelli *et al.* (1998) found that a two-term Henyey–Greenstein single-particle phase function provided a better fit than a one-term function to Viking Phobos data covering ~120° in phase angle.) We froze all shape and spin-state parameters, floated the Hapke parameters, and then fit only the data in blocks labeled "T", "N", and "D,W". The result was to decrease the rms error for these 34 data (that spanned ~ 4° of phase) only slightly from 0.094 mag to 0.084 mag, and this required a seemingly unphysical macroscopic roughness parameter $\overline{\theta} = 65°$.

The results discussed above suggest that much of the residual in these fits might be due to errors in the data of the type noted by Wisniewski (1993) in the Gaspra data set. On the other hand, there are examples where the model implies an offset between observations at the same observatory on consecutive days. For example, blocks "D,W" and "W" (between JD 2449009 and JD 2449011) include observations from the same observer on two consecutive nights, and the model predicts an offset of ~0.1 magnitude between these.

A more extreme case is that of the two "A" blocks on JD 2449013 and JD 2449014. (The former represents, by far, the largest residual in the entire fit.) The model predicts a significant lightcurve minimum near this time, and that the brightness should increase from the first block to the second. The observed data show quite the opposite. If the model is correct it implies an offset of about ~0.6 magnitude on consecutive nights at this observatory.

The possibility that these offset residuals might be real led us to examine inhomogeneous photometric functions. Simonelli *et al.* (1995) concluded that macroscopic roughness ($\overline{\theta}$) variations were a more likely explanation for Gaspra lightcurve residuals than albedo (w) variations. Hudson and Ostro (1997) found that $\overline{\theta}$ variations could reduce rms residuals for Castalia lightcurve fits but noted that in that case albedo variations could achieve a similar result.

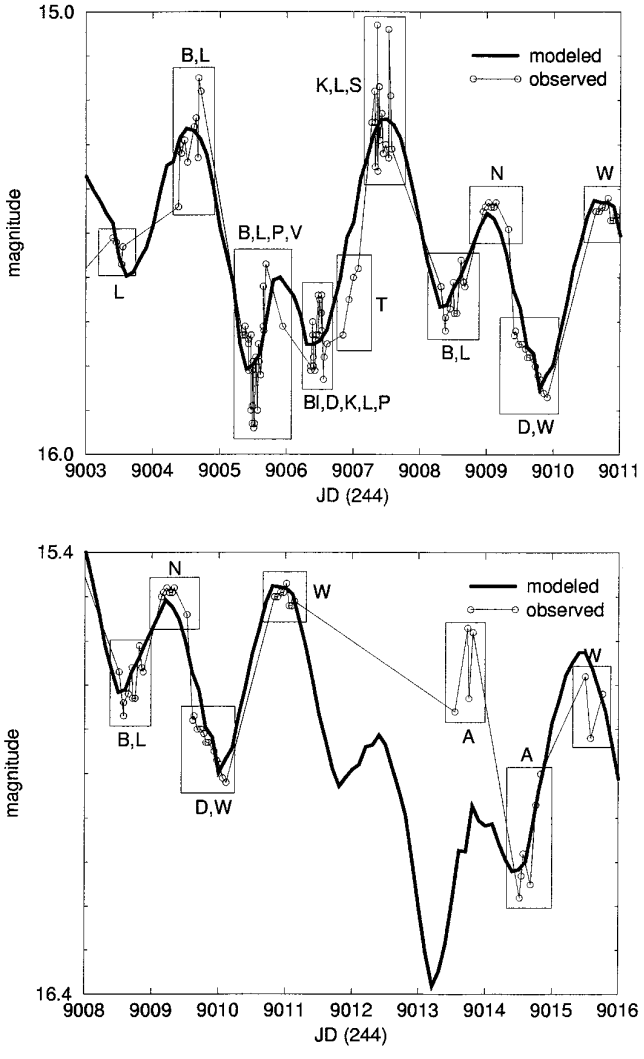

FIG. 3. Same as Fig. 2 but using an inhomogeneous photometric model.

We examined two inhomogeneous photometric models for Toutatis: one with a variable w and one with a variable $\overline{\theta}$. The $\overline{\theta}$ model was not effective in reducing the rms residual. This makes sense as much of the residual occurs near zero-phase, a situation in which the effects of shading (hence $\overline{\theta}$) are small. The w model was more effective, reducing the rms residual of the entire data set to 0.078 mag.

Figure 3 illustrates the nature of the inhomogeneous model fits. Generally the offset residuals are reduced, although the first "A" block remains an outlier. However, achieving this improvement requires a *very* inhomogeneous surface. The mean value of w is 0.27 and the standard

deviation is 0.19. Fractional albedo variations of this magnitude, far more than what has been observed on asteroids visited by spacecraft, do not seem plausible. We believe that the inhomogeneous model is simply using its much larger number of free parameters to fit residuals that in many cases likely represent calibration offsets between different observations.

Single Particle Scattering Properties

Toutatis's particle single-scattering albedo ($w = 0.26$) and phase-function asymmetry parameter ($g = -0.29$) are close to those determined for other S-class asteroids, consistent with its S-class designation (Howell *et al.* 1994).

Opposition Surge Parameters

In Hapke's development (Hapke 1993, Section 8.H) the opposition effect is due to shadow hiding. Theoretically it has an amplitude $B_0 = 1$, but values smaller than unity can be interpreted as a decrease in shadow-hiding due to multiple scattering, an effect that should increase with increasing particle albedo. For many asteroids, including Gaspra and Ida (Table II), estimates of B_0 exceed unity. Shadow hiding alone cannot account for $B_0 > 1$ so presumably some other effect is responsible. However, Helfenstein *et al.* (1997) have shown that for a wide variety of Solar System bodies, the relation

$$B_0 = 1.083[wp(0)]^{-0.629}, \quad (1)$$

with $p(0)$ the particle phase function at zero phase, gives a reasonable description of the dependence of B_0 on particle albedo for both $B_0 \leq 1$ and $B_0 > 1$, suggesting that a common process might be at work in both cases. For Toutatis $wp(0) = 0.668$ and Eq. (1) predicts $B_0 = 1.4$. The range of our estimate $B_0 = 1.20 \pm 0.32$ includes both 1.4 and unity.

A physical interpretation (Hapke 1986, 1993, see Section 8.H.3) of the opposition-surge width parameter is

$$h = -\frac{3}{8}\ln(P)Y, \quad (2)$$

where P is the porosity and Y is a function of the distribution of particle sizes. As h cannot uniquely constrain both P and Y, we combined radar porosity estimates with the h parameter to investigate constraints on the particle size distribution.

Ostro *et al.* (1998) used the physical model of Hudson and Ostro (1995) to analyze dual-polarization Goldstone radar images of Toutatis taken in 1996. They concluded that a significant fraction of Toutatis's surface must be covered with rock while the rest is blanketed with a regolith that is smooth at millimeter to meter scales. Using 4.9 g cm^{-3} as an upper bound of the intrinsic density of the surface material, they estimated that the porosity of the powdered component of Toutatis's surface is probably less than $P_{\max} = 0.6$. Therefore we estimate an upper bound on Y of

$$Y_{\max} = \left(\frac{8}{3}\right)\frac{0.036 + 0.023}{\ln(1/0.6)} = 0.31. \quad (3)$$

This value constrains the possible size distribution of particles. For example, it rules out a regolith of identically sized particles ($Y = 1$) or with a uniform size distribution ($Y = 0.77$). Following Hapke (1993, see Section 8.H.3) and assuming a ratio of largest to smallest particle sizes of 1000 (mm to μm), $Y = 0.31$ implies that if the particle sizes are governed by a power law $N(a) \propto a^{-\nu}$, then $1.2 \leq \nu \leq 4.2$. Consequently, the photometric behavior of Toutatis near opposition strongly implies that the ''smooth'' component of the surface is a powdered regolith with a significant fraction of microscopic particles.

Macroscopic Roughness

Helfenstein (1988) studied the relationship between topographic scale and photometric estimation of $\overline{\theta}$ and confirmed that $\overline{\theta}$ represents the combined effects of all scales of roughness up to the resolution limit of the photometry used in the estimation. In the present case, relief at scales larger than the resolution of our shape model (~100 m) are accounted for by the shape itself. Therefore we can interpret our value $\overline{\theta} = 32°$ as describing roughness at scales from tens of meters down to subcentimeter. Independent characterization of Toutatis's considerable roughness at centimeter to meter scales is provided by its relatively large radar circular polarization ratio $\mu_C \approx 0.3$ (Ostro *et al.*, unpublished results). It is possible that $\overline{\theta}$ is measuring roughness at this same scale and that Toutatis is smooth at scales of ~10 to ~100 m. However, given the object's irregular shape at scales above ~ 100 m, it seems more likely that the surface of Toutatis is very rough at all scales.

Helfenstein also noted that ''Hapke's equation does not accurately describe the photometric behavior at large incidence and phase angles of surfaces whose topographic values of $\overline{\theta}$ exceed about 10 degrees.'' Therefore, although Toutatis's $\overline{\theta} = 32°$ value implies that it is rougher than most other asteroids, a quantitative interpretation may not be possible.

ACKNOWLEDGMENTS

We are grateful to M. Belton, A. Harris, and reviewers D. Simonelli and R. Millis for their very helpful comments. Work at WSU was supported by NASA Grant NAGW-4636. Part of this research was conducted at the

Jet Propulsion Laboratory, California Institute of Technology, under contract with NASA.

REFERENCES

Bowell, E., B. Hapke, D. Domingue, K. Lumme, J. Peltoniemi, and A. W. Harris 1989. Application of photometric models to asteroids. In *Asteroids II* (R. P. Binzel, T. Gehrels, and M. S. Matthews, Eds.), pp. 524–556. Univ. of Arizona Press, Tucson.

Garvin, J. B., J. W. Head, G H. Pettengill, and S. H. Zisk 1985. Venus global radar reflectivity and correlations with elevation. *J. Geophy. Res.* **90,** 6859–6871.

Hapke, B. 1981. Bidirectional reflectance spectroscopy 1. Theory. *J. Geophys. Res.* **86,** 3039–3054.

Hapke, B. 1984. Bidirectional reflectance spectroscopy 3. Correction for macroscopic roughness *Icarus* **59,** 41–59.

Hapke, B. 1986. Bidirectional reflectance spectroscopy 4. The extinction coefficient and the opposition effect. *Icarus* **67,** 264–280.

Hapke, B. 1993. *Theory of Reflectance and Emittance Spectroscopy.* Cambridge Univ. Press, Cambridge, UK.

Helfenstein, P. 1988. The geological interpretation of photometric surface roughness. *Icarus* **73,** 462–481.

Helfenstein, P., J. Veverka, and J. Hillier 1997. The lunar opposition effect: A test of alternative models. *Icarus* **128,** 2–14.

Helfenstein, P., J. Veverka, P. C. Thomas, D. P. Simonelli, K. Klaasen, T. V. Johnson, F. Fanale, J. Granahan, A. S. McEwen, M. Belton, and C. Chapman 1996. Galileo photometry of asteroid 243 Ida. *Icarus* **120,** 48–65.

Helfenstein, P., J. Veverka, P. C. Thomas, D. P. Simonelli, P. Lee, K. Klaasen, T. V. Johnson, H. Breneman, J. W. Head, S. Murchie, F. Fanale, M. Robinson, B. Clark, J. Granahan, H. Garbeil, A. S. McEwen, R. L. Kirk, M. Davies, G. Neukum, S. Mottola, R. Wagner, M. Belton, C. Chapman, and C. Pilcher 1994. Galileo photometry of asteroid 951 Gaspra. *Icarus* **107,** 37–60.

Howell, E. S., D. T. Britt, J. F. Bell, R. P. Binzel, and L. A. Lebofsky 1994. Visible and near-infared spectral observations of 4179 Toutatis. *Icarus* **111,** 468–474.

Hudson, R. S., and S. J. Ostro 1994. Shape of asteroid 4769 Castalia (1989 PB) from inversion of radar images. *Science* **263,** 940–943.

Hudson, R. S., and S. J. Ostro 1995. Shape and non-principal axis spin state of asteroid 4179 Toutatis. *Science* **270,** 84–86.

Hudson, R. S., S. J. Ostro, and A. W. Harris 1997. Constraints on spin state and Hapke parameters of asteroid 4769 Castalia using lightcurves and a radar-derived shape model. *Icarus* **130,** 165–176.

Landau, L. D., and E. M. Lifshitz 1976. *Mechanics,* 3rd ed. Pergamon, Oxford.

Ostro, S. J., R. S. Hudson, R. F. Jurgens, K. D. Rosema, D. B. Campbell, D. K. Yeomans, J. F. Chandler, J. D. Giorgini, R. Winkler, R. Rose, S. D. Howard, M. A. Slade, P. Perillat, and I. I. Shapiro 1995. Radar images of asteroid 4179 Toutatis. *Science* **270,** 80–83.

Simonelli, D. P., J. Veverka, P. C. Thomas, and P. Helfenstein 1995. Analysis of Gaspra lightcurves using Galileo shape and photometric models. *Icarus* **114,** 387–402.

Simonelli, D. P., J. Veverka, P. C. Thomas, and P. Helfenstein, B. T. Carcich, and M. J. S. Belton 1996. Ida lightcurves: Consistency with Galileo shape and photometric models. *Icarus* **120,** 38–47.

Simonelli, D. P., M. Wisz, A. Switala, D. Adinolfi, J. Veverka, P. C. Thomas, and P. Helfenstein 1998. Photometric properties of Phobos surface materials from Viking images. *Icarus* **131,** 52–77.

Spencer, J. R., and 47 colleagues 1995. The lightcurve of 4179 Toutatis: Evidence for complex rotation. *Icarus* **117,** 71–89.

Thomas, P. C., J. Veverka, D. Simonelli, P. Helfenstein, B. Carcich, M. J. S. Belton, M. E. Davies, and C. Chapman 1994. The shape of Gaspra. *Icarus* **107,** 23–36.

Thomas, P. C., M. J. S. Belton, B. Carcich, C. R. Chapman, M. E. Davies, R. Sullivan, and J. Veverka 1996a. The shape of Ida. *Icarus* **120,** 20–32.

Thomas, P. C., D. Adinolfi, P. Helfenstein, D. Simonelli, and J. Veverka 1996b. The surface of Deimos: Contribution of materials and processes to its unique appearance. *Icarus* **123,** 536–556.

Veverka, J. 1977. The physical meaning of phase coefficients. In *Physical Studies of Minor Planets* (T. Gehrels, Ed.). NASA SP-267, U. S. Govt. printing Office, pp. 79–90.

Whipple, A. L., and P. J. Shelus 1993. Long-term dynamical evolution of the minor planet (4179) Toutatis. *Icarus* **105,** 408–419.

Wisniewski, W. Z., and 21 colleagues 1993. Ground-based photometry of Asteroid 951 Gaspra. *Icarus* **101,** 213–222.

Yeomans, D. K., and P. W. Chodas 1994. Predicting close approaches of asteroids and comets to Earth. In *Hazards Due to Comets and Asteroids* (Gehrels, T., Ed.) pp. 241–258. Univ. of Arizona Press, Tucson.